Physics Letters B 668 (2008) 187–192

Contents lists available at ScienceDirect

Physics Letters B

www.elsevier.com/locate/physletb

# Proton–proton fusion in pionless effective theory

S. Ando [a,b,*], J.W. Shin [a], C.H. Hyun [c], S.W. Hong [a], K. Kubodera [d]

[a] *Department of Physics, Sungkyunkwan University, Suwon 440-746, South Korea*
[b] *Theoretical Physics Group, School of Physics and Astronomy, The University of Manchester, Manchester, M13 9PL, UK*
[c] *Department of Physics Education, Daegu University, Gyeongsan 712-714, South Korea*
[d] *Department of Physics and Astronomy, University of South Carolina, Columbia, SC 29208, USA*

ARTICLE INFO

*Article history:*
Received 30 January 2008
Accepted 19 August 2008
Available online 28 August 2008
Editor: W. Haxton

*PACS:*
21.45.Bc
26.20.Cd
26.65.+t

ABSTRACT

The proton–proton fusion reaction, $pp \to de^+\nu$, is studied in pionless effective field theory (EFT) with di-baryon fields up to next-to leading order. With the aid of the di-baryon fields, the effective range corrections are naturally resummed up to the infinite order and thus the calculation is greatly simplified. Furthermore, the low-energy constant which appears in the axial-current-di-baryon–di-baryon contact vertex is fixed through the ratio of two- and one-body matrix elements which reproduces the tritium lifetime very precisely. As a result we can perform a parameter free calculation for the process. We compare our numerical result with those from the accurate potential model and previous pionless EFT calculations, and find a good agreement within the accuracy better than 1%.



## 1. Introduction

The proton–proton fusion process, $pp \to de^+\nu_e$, is a fundamental reaction for the nuclear astrophysics, especially important for the understanding of the star evolutions [1] and solar neutrinos [2–4]. However, the process has never been studied experimentally because the event is extremely unlikely to take place in the laboratory at the proton energies in the sun. The calculation of the transition rate and its uncertainty has naturally become a challenge to nuclear theory. The first calculation of the process was carried out by Bethe and Critchfield [5] in 1938. This estimation was improved by Salpeter [6][1] in 1952. Later, small corrections, such as the electromagnetic radiative corrections, were considered by Bahcall and his collaborators [8,9] in the framework of effective range theory. Recently, accurate phenomenological potential models were employed to study the process [10,11]. Furthermore, in Ref. [12] the two-nucleon current operators were calculated from heavy-baryon chiral perturbation theory (HB$\chi$PT) up to next-to-next-to-next-to leading order (N$^3$LO), and Park et al. obtained quite an accurate estimation ($\sim 0.3\%$ uncertainty) for the process by fixing an unknown parameter, so-called low energy constant (LEC), which appears in the two-nucleon-axial-current contact interaction in terms of the tritium lifetime [13,14].

The kinetic energy relevant to the $pp$ fusion process at the core of the sun is quite low, $kT_c \simeq 1.18$ keV, where $T_c$ is the core temperature of the sun, $T_c \simeq 13.7 \times 10^6$ K, and $k$ is the Boltzmann constant. The proton momentum at the core, $p_c \simeq \sqrt{2m_p kT_c} \simeq$ 1.5 MeV, where $m_p$ is the proton mass, is still significantly small compared to the pion mass, $m_\pi \simeq 140$ MeV. Therefore, we may regard the pion as a heavy degree of freedom for the $pp$ fusion process. It may be convenient and suitable to employ a pionless effective field theory (EFT) [15], in which the pions are integrated out of the effective Lagrangian for the process in question. The $pp$ fusion process in the pionless theory has been studied by Kong and Ravndal [16] up to next-to leading order (NLO) and by Butler and Chen [17] up to fifth order (N$^4$LO). Thanks to the perturbative scheme in EFT, the accuracy of the N$^4$LO calculation would, in principle, be $(Q/\Lambda)^4 \sim (1/3)^4 \simeq 1\%$, where $Q/\Lambda \sim 1/3$ is a typical expansion parameter in the pionless theory. However, because of lack of the experimental data to fix an unknown LEC $L_{1A}$ which appears in the two-nucleon-axial-current contact interaction in the pionless effective Lagrangian, an uncertainty estimated in the pionless EFT for the $pp$ fusion process is still significantly larger than what is expected from the counting rules of the theory.

In this work, we employ a pionless EFT with di-baryon fields [18–20].[2] The amplitude for the $pp$ fusion process at the zero proton momentum is calculated up to NLO. We introduce two di-baryon fields [24], which have the same quantum numbers as those of $S$-wave two-nucleon states ($^1S_0$ and $^3S_1$ states), as auxiliary fields: after integrating out the di-baryon fields we do have

* Corresponding author at: Theoretical Physics Group, School of Physics and Astronomy, The University of Manchester, Manchester, M13 9PL, UK.
*E-mail address:* shung-ichi.ando@manchester.ac.uk (S. Ando).

[1] For a recent historical review, see Ref. [7].

[2] We have employed the same formalism in the studies of the two-body processes, such as neutron-neutron fusion [21], radiative neutron capture on a proton at BBN energies [22], and neutral pion production in proton–proton collision near threshold [23].

0370-2693/$ – see front matter © 2008 Published by Elsevier B.V.
doi:10.1016/j.physletb.2008.08.040

the ordinary pionless theory without the di-baryon fields. However, as have intensively been discussed in Refs. [18,19,25,26], with the aid of the di-baryon fields, resummation of the effective range correction up to the infinite order is naturally introduced, which greatly simplifies the calculation of higher order corrections to the wave functions. In addition, the new counting rules make the expansion parameter $Q$ much improved, and it is not necessary to employ the power divergence subtraction scheme [27] any longer. Furthermore, by assuming that the leading order (LO) contribution in the di-baryon–di-baryon-current contact interaction can be determined mainly from the one-body current interaction as discussed in Ref. [19], we can reproduce the results from the effective range theory [28] in the LO calculations of the pionless EFT with the di-baryon fields. The NLO correction, the di-baryon–di-baryon-current contact interaction denoted by the unknown LEC $l_{1A}$, is approximately presumed to be the two-body (2B) current correction in the pionful calculations. We fix the LEC $l_{1A}$ by using the relative strength of the two-body matrix element to that of the one-body contribution, $\delta_{2B}$ [14], which has been determined from the accurate tritium lifetime datum. (We discuss it in detail later.) Consequently we can make our estimation of the $pp$ fusion amplitude free from unknown parameters. Moreover, though our calculation is rather simple and is only up to NLO, we can obtain a result comparable to that from the accurate potential model calculation within the accuracy better than $\sim 1\%$.

This Letter is organized in the followings: in Section 2, we introduce the pionless effective Lagrangian with the di-baryon fields up to NLO, and in Section 3, we fix the LECs which appear in the initial and final two-nucleon states by using the effective range parameters. In Section 4, the amplitude for the $pp$ fusion process is calculated up to NLO. We show our numerical results in Section 5. In Section 6, discussion and conclusions are given.

## 2. Pionless effective Lagrangian with di-baryon fields

For the low-energy process, the weak-interaction Hamiltonian can be taken to be

$$\mathcal{H} = \frac{G_F V_{ud}}{\sqrt{2}} l_\mu J^\mu, \tag{1}$$

where $G_F$ is the Fermi constant and $V_{ud}$ is the CKM matrix element. $l_\mu$ is the lepton current $l_\mu = \bar{u}_e \gamma_\mu (1-\gamma_5) v_\nu$, and $J_\mu$ is the hadronic current. We will calculate the two-body hadronic current $J^\mu$ from the pionless effective Lagrangian with di-baryon fields up to NLO.

We adopt the standard counting rules of pionless EFT with di-baryon fields [18]. Introducing an expansion scale $Q < \Lambda (\simeq m_\pi)$, we count the magnitude of spatial part of the external and loop momenta, $|\vec{p}|$ and $|\vec{l}|$, as $Q$, and their time components, $p^0$ and $l^0$, as $Q^2$. The nucleon and di-baryon propagators are of $Q^{-2}$, and a loop integral carries $Q^5$. The scattering lengths and effective ranges are counted as $Q \sim \{\gamma, 1/a_0, 1/\rho_d, 1/r_0\}$ where $\gamma$, $a_0$, $\rho_d$ and $r_0$ are the effective range parameters for the $S$-wave $NN$ scattering; $\gamma \equiv \sqrt{m_N B}$, where $B$ is the deuteron binding energy, $a_0$ is the scattering length in the ${}^1S_0$ channel, $\rho_d$ and $r_0$ are the effective ranges in the ${}^3S_1$ and ${}^1S_0$ channel, respectively. The orders of vertices and transition amplitudes are easily obtained by counting the numbers of these factors in the Lagrangian and diagrams, respectively. As discussed below, some vertices acquire factors like $r_0$ and $\rho_d$ after renormalization and thus their orders can differ from what the above naive dimensional analysis suggests. Note that we do not include the higher order radiative corrections, such as the vacuum polarization effect [29] and the radiative corrections from one-body part [30].

A pionless effective Lagrangian with di-baryon fields may be written as [18,19]

$$\mathcal{L} = \mathcal{L}_N + \mathcal{L}_s + \mathcal{L}_t + \mathcal{L}_{st}, \tag{2}$$

where $\mathcal{L}_N$ is a one-nucleon Lagrangian, $\mathcal{L}_s$ is the spin-singlet (${}^1S_0$ state) di-baryon Lagrangian including coupling to the two-nucleon, $\mathcal{L}_t$ is the spin-triplet (${}^3S_1$ state) di-baryon Lagrangian including coupling to the two-nucleon and $\mathcal{L}_{st}$ describes the weak-interaction transition (due to the axial current) from the ${}^1S_0$ di-baryon to the ${}^3S_1$ di-baryon.

A pionless one-nucleon Lagrangian in the heavy-baryon formalism reads

$$\mathcal{L}_N = N^\dagger \left\{ iv\cdot D - 2ig_A S\cdot\Delta + \frac{1}{2m_N}\left[(v\cdot D)^2 - D^2\right] + \cdots \right\} N, \tag{3}$$

where the ellipsis represents terms that do not appear in this calculation. $v^\mu$ is the velocity vector satisfying $v^2 = 1$; we choose $v^\mu = (1, \vec{0})$, and $S^\mu$ is the spin operator $2S^\mu = (0, \vec{\sigma})$. Covariant derivative $D_\mu$ reads as $D_\mu = \partial_\mu - \frac{i}{2}\vec{\tau}\cdot\vec{\mathcal{V}}_\mu$ where $\vec{\mathcal{V}}_\mu$ is the external isovector vector current, and $\Delta_\mu = -\frac{i}{2}\vec{\tau}\cdot\vec{\mathcal{A}}_\mu$, where $\vec{\mathcal{A}}_\mu$ is the external isovector axial current. $g_A$ is the axial-vector coupling constant and $m_N$ is the nucleon mass.

The Lagrangians that involve the di-baryon fields are given by

$$\begin{aligned}\mathcal{L}_s &= \sigma_s s_a^\dagger \left[ iv\cdot D + \frac{1}{4m_N}\left[(v\cdot D)^2 - D^2\right] + \Delta_s \right] s_a \\ &\quad - y_s\left[s_a^\dagger\left(N^T P_a^{({}^1S_0)} N\right) + \text{h.c.}\right], \end{aligned}\tag{4}$$

$$\begin{aligned}\mathcal{L}_t &= \sigma_t t_i^\dagger \left[ iv\cdot D + \frac{1}{4m_N}\left[(v\cdot D)^2 - D^2\right] + \Delta_t \right] t_i \\ &\quad - y_t\left[t_i^\dagger\left(N^T P_i^{({}^3S_1)} N\right) + \text{h.c.}\right], \end{aligned}\tag{5}$$

$$\mathcal{L}_{st} = -\left[\left(\frac{r_0 + \rho_d}{2\sqrt{r_0\rho_d}}\right) g_A + \frac{l_{1A}}{m_N\sqrt{r_0\rho_d}}\right]\left[s_a^\dagger t_i \mathcal{A}_i^a + \text{h.c.}\right], \tag{6}$$

where $s_a$ and $t_i$ are the di-baryon fields for the ${}^1S_0$ and ${}^3S_1$ channel, respectively. The covariant derivative for the di-baryon field is given by $D_\mu = \partial_\mu - iC\mathcal{V}_\mu^{\text{ext}}$ where $\mathcal{V}_\mu^{\text{ext}}$ is the external vector field. $C$ is the charge operator for the di-baryon field; $C = 0, 1, 2$ for the $nn$, $np$, $pp$ channel, respectively. $\sigma_{s,t}$ is the sign factor $\sigma_{s,t} = \pm 1$ and $\Delta_{s,t}$ is the mass difference between the di-baryon and two nucleons, $m_{s,t} = 2m_N + \Delta_{s,t}$. $y_{s,t}$ is the di-baryon–two-nucleon coupling constant. $P_i^{(S)}$ is the projection operator for the $S = {}^1S_0$ or ${}^3S_1$ channel;

$$\begin{aligned} &P_a^{({}^1S_0)} = \frac{1}{\sqrt{8}}\sigma_2\tau_2\tau_a, \qquad P_i^{({}^3S_1)} = \frac{1}{\sqrt{8}}\sigma_2\sigma_i\tau_2, \\ &\text{Tr}\left(P_i^{(S)\dagger} P_j^{(S)}\right) = \frac{1}{2}\delta_{ij}, \end{aligned}\tag{7}$$

where $\sigma_i$ ($\tau_a$) is the spin (isospin) operator. Note that, as mentioned in the Introduction, we separate the di-baryon–di-baryon-current contact interaction in Eq. (6) into the LO and NLO terms. The LO interaction proportional to $g_A$ is determined by the one-body axial-current interaction and the factor $\frac{1}{2}(r_0+\rho_d)/\sqrt{r_0\rho_d}$ is included so as to reproduce the result from the effective range theory at LO. The NLO correction is parameterized by the LEC $l_{1A}$. More detailed discussion about the separation of LO and NLO contact interaction with external probe in the di-baryon formalism can be found in Ref. [19].

## 3. Initial and final $NN$ channels

The typical energy of the $pp$ fusion reaction is very low, as discussed in the Introduction, so we can assume that the dominant channel of the reaction is from the initial ${}^1S_0$ $pp$ state to the final

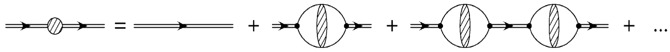

**Fig. 1.** Diagrams for the dressed di-baryon propagator including the Coulomb interaction. A double-line with a filled circle denotes the renormalized dressed di-baryon propagator. Double-lines without the filled circle and single-curves denote the bare di-baryon propagators and nucleon propagators, respectively. Two-nucleon propagator with a shaded blob denotes the Green's function including the Coulomb potential. A (spin-singlet) di-baryon–nucleon–nucleon ($sNN$) vertex is proportional to the LEC $y_s$.

$^3S_1$ deuteron state. In this section, we fix the LECs which appear in the initial and final two-nucleon states for the $pp$ fusion process from the effective range parameters.

In Fig. 1, LO diagrams for the initial $pp$ state in $^1S_0$ channel, i.e., the dressed $^1S_0$ channel di-baryon propagator, are shown where the two-nucleon bubble diagrams including the Coulomb interaction are summed up to the infinite order. The inverse of the propagator in the center of mass (CM) frame is thus obtained by

$$iD_s^{-1}(p) = i\sigma_s(E+\delta_s) - iy_s^2 J_0(p), \tag{8}$$

with

$$J_0(p) = \int \frac{d^3\vec{k}}{(2\pi)^3}\frac{d^3\vec{q}}{(2\pi)^3}\langle\vec{q}|\hat{G}_C^{(+)}(E)|\vec{k}\rangle, \tag{9}$$

where $\hat{G}_C^{(+)}$ is the outgoing two-nucleon Green's function including the Coulomb potential,

$$\hat{G}_C^{(+)}(E) = \frac{1}{E-\hat{H}_0-\hat{V}_C+i\epsilon}. \tag{10}$$

$E$ is the total CM energy, $E \simeq p^2/m_N$, $\hat{H}_0$ is the free Hamiltonian for two-proton, $\hat{H}_0 = \hat{p}^2/m_N$, and $\hat{V}_C$ is the repulsive Coulomb force $\hat{V}_C = \alpha/r$: $\alpha$ is the fine structure constant. Employing the dimensional regularization in $d = 4-2\epsilon$ space–time dimension, we obtain [31,32]

$$J_0(p) = \frac{\alpha m_N^2}{8\pi}\left[\frac{1}{\epsilon} - 3C_E + 2 + \ln\left(\frac{\pi\mu^2}{\alpha^2 m_N^2}\right)\right] - \frac{\alpha m_N^2}{4\pi}h(\eta) - C_\eta^2\frac{m_N}{4\pi}(ip), \tag{11}$$

where $\mu$ is the scale of the dimensional regularization, $C_E = 0.5772\ldots$, and

$$h(\eta) = \mathrm{Re}\,\psi(i\eta) - \ln\eta, \quad \mathrm{Re}\,\psi(\eta) = \eta^2\sum_{\nu=1}^{\infty}\frac{1}{\nu(\nu^2+\eta^2)} - C_E,$$

$$C_\eta^2 = \frac{2\pi\eta}{e^{2\pi\eta}-1}, \quad \eta = \frac{\alpha m_N}{2p}. \tag{12}$$

Thus the inverse of renormalized dressed di-baryon propagator is obtained as

$$iD_s^{-1}(p) = iy_s^2\frac{m_N}{4\pi}\left[\frac{4\pi\sigma_s\Delta_s^R}{m_N y_s^2} + \frac{4\pi\sigma_s}{m_N^2 y_s^2}p^2 + \alpha m_N h(\eta) + ipC_\eta^2\right], \tag{13}$$

where $\Delta_s^R$ is the renormalized mass difference

$$\sigma_s\Delta_s^R = \sigma_s\Delta_s - y_s^2\frac{\alpha m_N^2}{8\pi}\left[\frac{1}{\epsilon} - 3C_E + 2 + \ln\left(\frac{\pi\mu^2}{\alpha^2 m_N^2}\right)\right]. \tag{14}$$

In Fig. 2, a diagram of the $S$-wave $pp$ scattering amplitude with the Coulomb and strong interactions is shown. Thus we have the $S$-wave scattering amplitude as

$$iA_s = (-iy_s\psi_0)iD_s(p)(-iy_s\psi_0) = i\frac{4\pi}{m_N}\frac{C_\eta^2 e^{2i\sigma_0}}{-\frac{4\pi\sigma_s\Delta_s^R}{m_N y_s^2} - \frac{4\pi\sigma_s p^2}{m_N^2 y_s^2} - \alpha m_N h(\eta) - ipC_\eta^2}, \tag{15}$$

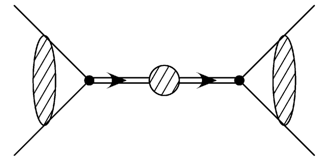

**Fig. 2.** Diagram for the $S$-wave $pp$ scattering amplitude with the Coulomb and strong interactions. See the caption of Fig. 1 for details.

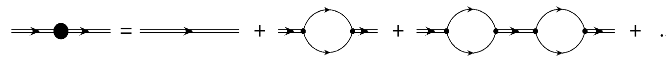

**Fig. 3.** Dressed di-baryon propagator without Coulomb interaction (double line with a filled circle) at leading order. A single line stands for the nucleon, while a double line represents the bare di-baryon.

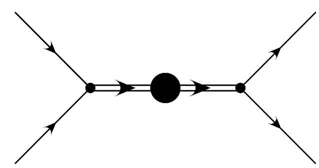

**Fig. 4.** Diagram for the $S$-wave $NN$ amplitude without Coulomb interaction at leading order. The double line with a filled circle represents the dressed di-baryon propagator obtained in Fig. 3.

with

$$\psi_0 = \int\frac{d^3\vec{k}}{(2\pi)^3}\langle\vec{k}|\psi_{\vec{p}}^{(+)}\rangle = \int\frac{d^3\vec{k}}{(2\pi)^3}\langle\psi_{\vec{p}}^{(-)}|\vec{k}\rangle = C_\eta e^{i\sigma_0}, \tag{16}$$

where $\langle\vec{k}|\psi_{\vec{p}}^{(\pm)}\rangle$ are the Coulomb wave functions obtained by solving the Schrödinger equations $(\hat{H}-E)|\psi_{\vec{p}}^{(\pm)}\rangle = 0$ with $\hat{H} = \hat{H}_0 + \hat{V}_C$ and represented in the $|\vec{k}\rangle$ space for the two protons. $\sigma_0$ is the $S$-wave Coulomb phase shift $\sigma_0 = \arg\Gamma(1+i\eta)$. The $S$-wave amplitude $A_s$ is given in terms of the effective range parameters as

$$iA_s = i\frac{4\pi}{m_N}\frac{C_\eta^2 e^{2i\sigma_0}}{-\frac{1}{a_C} + \frac{1}{2}r_0p^2 + \cdots - \alpha m_N h(\eta) - ipC_\eta^2}, \tag{17}$$

where $a_C$ is the scattering length, $r_0$ is the effective range, and the ellipsis represents the higher order effective range corrections. Now it is easy to match the parameters $\sigma_s$ and $y_s$ with the effective range parameters. Thus we have $\sigma_s = -1$ and

$$y_s = \pm\frac{2}{m_N}\sqrt{\frac{2\pi}{r_0}},$$

$$D_s(p) = \frac{m_N r_0}{2}\frac{1}{\frac{1}{a_C} - \frac{1}{2}r_0p^2 + \alpha m_N h(\eta) + ipC_\eta^2}. \tag{18}$$

In Fig. 3, LO diagrams for the final deuteron channel, i.e., the dressed $^3S_1$ channel di-baryon propagators are depicted. Since insertion of a two-nucleon one-loop diagram does not alter the order of the diagram, the two-nucleon bubbles should be summed up to the infinite order. Thus the inverse of the dressed di-baryon propagator for the deuteron channel in the CM frame reads

$$iD_t^{-1}(p) = i\sigma_t(E+\Delta_t) + iy_t^2\frac{m_N}{4\pi}(ip) = i\frac{m_N y_t^2}{4\pi}\left[\frac{4\pi\sigma_t\Delta_t}{m_N y_t^2} + \frac{4\pi\sigma_t E}{m_N y_t^2} + ip\right], \tag{19}$$

where we have used dimensional regularization for the loop integral and $E$ is the total energy of the two nucleons, $E \simeq p^2/m_N$. The dressed di-baryon propagators are renormalized via the $S$-wave

$NN$ amplitudes. The amplitudes obtained from the diagram in Fig. 4 should satisfy

$$iA_t = (-iy_t)\big[iD_t(p)\big](-iy_t) = \frac{4\pi}{m_N}\frac{i}{-\frac{4\pi\sigma_t\Delta_t}{m_N y_t^2} - \frac{4\pi\sigma_t}{m_N y_t^2}p^2 - ip}, \tag{20}$$

where $A_t$ is related to the $S$-wave $NN$ scattering $S$-matrix via

$$S - 1 = e^{2i\delta_t} - 1 = \frac{2ip}{p\cot\delta_t - ip} = i\left(\frac{pm_N}{2\pi}\right)A_t. \tag{21}$$

Here $\delta_t$ is the phase shift for the $^3S_1$ channel. Meanwhile, effective range expansion reads

$$p\cot\delta_t = -\gamma + \frac{1}{2}\rho_d\big(\gamma^2 + p^2\big) + \cdots. \tag{22}$$

Now, the above renormalization condition allows us to relate the LECs to the effective-range expansion parameters. For the deuteron channel, one has $\sigma_t = -1$ and

$$y_t = \pm\frac{2}{m_N}\sqrt{\frac{2\pi}{\rho_d}},$$

$$D_t(p) = \frac{m_N\rho_d}{2}\frac{1}{\gamma + ip - \frac{1}{2}\rho_d(\gamma^2 + p^2)} = \frac{Z_d}{E+B} + \cdots, \tag{23}$$

where $Z_d$ is the wave function normalization factor of the deuteron at the pole $E = -B$, and the ellipsis in Eq. (23) denotes corrections that are finite or vanish at $E = -B$. Thus one has [18]

$$Z_d = \frac{\gamma\rho_d}{1 - \gamma\rho_d}. \tag{24}$$

This $Z_d$ is equal to the asymptotic $S$-state normalization constant. It is to be noted that the order of the LECs $y_t$ is now of $Q^{1/2}$, and the deuteron state is also described by the renormalized dressed di-baryon propagator.

## 4. Amplitude up to NLO

Diagrams for the $pp$ fusion process up to NLO are shown in Fig. 5. In the limit $p \to 0$, we have the amplitude from the diagrams in the figure as

$$A = -\vec{\epsilon}^{\,*}_{(d)} \cdot \vec{\epsilon}_{(l)} G_F V_{ud} g_A T_{fi}. \tag{25}$$

Here $\vec{\epsilon}^{\,*}_{(d)}$ is the spin polarization vector of the out-going deuteron, $\vec{\epsilon}_{(l)}$ is the spatial part of the lepton current $l^\mu$ in Eq. (1), and

$$T_{fi} \simeq \sqrt{\frac{8\pi\gamma}{1-\gamma\rho_d}}\frac{C_\eta e^{i\sigma_0}}{\gamma^2}\bigg[e^\chi - a_C\gamma\chi I(\chi) + \frac{1}{4}a_C(r_0 + \rho_d)\gamma^2 + \frac{a_C\gamma^2}{2g_A m_p}l_{1A}\bigg], \tag{26}$$

where

$$I(\chi) = \frac{1}{\chi} - e^\chi E_1(\chi), \quad E_1(\chi) = \int_\chi^\infty dt\frac{e^{-t}}{t}, \tag{27}$$

with $\chi = \alpha m_p/\gamma$. We note that the amplitude $T_{fi}$ vanishes at the $p \to 0$ limit because of the overall factor $C_\eta$. The approximation is taken by keeping $p$ dependence in $C_\eta$ while ignoring higher order $p/m_N$ corrections in the remaining part. Since $p/m_N \sim 0.2\%$, the contribution from the higher order $p/m_N$ terms will be sub 1% order, which can be neglected conservatively at the uncertainty level we are considering in the present work. Introducing a "standard reduced matrix element" [16],

$$\Lambda(p) = \sqrt{\frac{\gamma^3}{8\pi C_\eta^2}}\big|T_{fi}(p)\big|, \tag{28}$$

we have a finite and analytic expression of the reduced matrix element $\Lambda(p)$ in the $p \to 0$ limit as

$$\Lambda(0) = \frac{1}{\sqrt{1-\gamma\rho_d}}\bigg\{e^\chi - a_C\gamma\big[1 - \chi e^\chi E_1(\chi)\big] + \frac{1}{4}a_C(r_0+\rho_d)\gamma^2 + \frac{a_C\gamma^2}{2g_A m_p}l_{1A}\bigg\}. \tag{29}$$

As mentioned above, we exactly reproduce the result of the effective range theory at LO, and have a higher order correction proportional to the LEC $l_{1A}$ at NLO in Eq. (29).

## 5. Numerical results

We obtain the matrix element $\Lambda(0)$ in Eq. (29) in terms of the four effective range parameters, $a_C$, $r_0$, $\gamma$ and $\rho_d$, and the LEC $l_{1A}$. The values of the effective range parameters are well known, but three of them are slightly different in the references. In this work, we take two sets of the values: one is $a_C = -7.8063 \pm 0.0026$ fm, $r_0 = 2.794 \pm 0.014$ fm, and $\rho_d = 1.760 \pm 0.005$ fm from Table VIII in Ref. [33]. The other is $a_C = -7.8149 \pm 0.0029$ fm, $r_0 = 2.769 \pm 0.014$ fm, and $\rho_d = 1.753 \pm 0.008$ fm from Table XIV in Ref. [34]. We take an average of numerical values of $\Lambda(0)$ from the two sets of the parameters for our numerical result. The value of the LEC $l_{1A}$ should be fixed by experimental data, but there are no precise ones for the two-body system. We fix the value of the LEC $l_{1A}$ indirectly from the relative strength of the two-body matrix element to one-body one, $\delta_{2B} \equiv \mathcal{M}_{2B}/\mathcal{M}_{1B} = (0.86 \pm 0.05)\%$ in Eq. (29) in Ref. [14]. This value has been obtained from the accurate potential model calculation for the two-body matrix element with the current operators derived from HB$\chi$PT up to N$^3$LO where the two-body current operator has been fixed from an accurate experimental datum, the tritium lifetime, for the three-body system. Thus we have

$$l_{1A} = -0.50 \pm 0.03, \tag{30}$$

where we have used our LO amplitude as the one-body input. This is a good approximation because the difference between the amplitude from the effective range theory, which is almost the same as our LO result, and that from accurate potential model calculations is tiny [12]. For other well known parameters, we use $B = 2.224575$ MeV, $g_A = 1.2695$, $m_p = 938.272$ MeV, and $m_n = 939.565$ MeV, and thus have $\gamma = 45.70$ MeV, $\chi = 0.1498$, and $E_1(\chi) = 1.465$.

Employing the values of the parameters mentioned above, we have $\Lambda_{\mathrm{LO}}(0) = 2.641$ at LO, and $\Lambda_{\mathrm{NLO1}}(0) = 2.662 \pm 0.002$ from

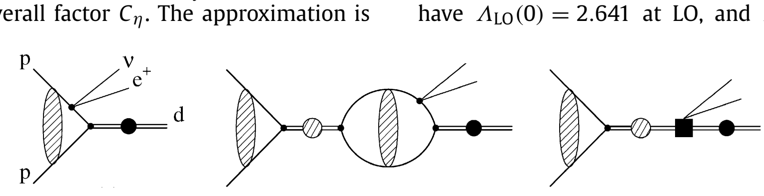


**Fig. 5.** Diagrams for the $pp$ fusion process, $pp \to de^+\nu_e$, up to NLO.

**Table 1**
Estimated values of $\Lambda^2(0)$. The value in second column is our result. The values in third, fourth, and fifth column are estimated from the pionless EFT calculation up to NLO by Kong and Ravndal (KR) [16], that up to N$^4$LO by Butler and Chen (BC) [17], and an accurate phenomenological potential model calculation [11], respectively

| | Our result | KR(NLO) [16] | BC(N$^4$LO) [17] | Pot. model [11] |
|---|---|---|---|---|
| $\Lambda^2(0)$ | $7.09 \pm 0.02$ | $7.04 \sim 7.70$ | $6.71 \sim 7.03$ | $7.05 \sim 7.06$ |

the first set of the parameter values and $\Lambda_{\mathrm{NLO2}}(0) = 2.664 \pm 0.003$ from the second one up to NLO. Thus we have an average value

$$\Lambda_{\mathrm{NLO}}(0) = 2.663 \pm 0.004, \tag{31}$$

and $\Lambda^2_{\mathrm{NLO}}(0) = 7.09 \pm 0.02$ where the estimated error bars mainly come from those of the effective ranges, $r_0$ and $\rho_d$, and the LEC $l_{1A}$.

In Table 1, we compare our numerical result for $\Lambda^2(0)$ with those from other theoretical estimations, the pionless EFT without di-baryons up to NLO by Kong and Ravndal (KR) [16], that up to N$^4$LO by Butler and Chen (BC) [17], and the accurate phenomenological potential model calculation [11]. We find that our numerical result is in good agreement with the values from the former theoretical estimations within the accuracy less than 1%. As discussed before, the uncertainties of the estimations from the pionless EFT without di-baryon fields are still large, ∼4.5% for the KR's estimation up to NLO, and ∼2.3% for the BC's one up to N$^4$LO, mainly because of the unfixed LEC $L_{1A}$. Though the results in the previous pionless EFT calculations have the unfixed LEC $L_{1A}$, we can directly compare our result of the amplitude $\Lambda(0)$ in Eq. (29) to the expressions in Eq. (7) in Ref. [17], and fix the value of the LEC $L_{1A}$. Assuming the higher order LEC $\bar{K}_{1A} = 0$, we have $L_{1A} = 1.27 \pm 0.12$ fm$^3$, which is consistent with our previous estimation, $L_{1A} = 1.18 \pm 0.11$ fm$^3$ in Ref. [21]. When comparing our result with that from the accurate phenomenological potential model calculation, we find that our result is overestimated by ∼0.5% mainly because we have not included the important contribution from the vacuum polarization effect.

As a last remark we would like to note that the precedent pionless EFT calculations include the higher order corrections in both wave functions and vertices with external probe. The contribution to $\Lambda(0)$ from the wave functions read 2.51, 2.54 and 2.58 at LO, NLO and N$^4$LO, respectively. In our calculation with di-baryon field, higher order corrections to the wave functions are incorporated naturally by the summation of effective range contribution to infinite order, which gives $\Lambda(0)$ equal to 2.64. A great advantage of the pionless EFT with di-baryon field lies in that we do not need to care the higher order contribution to the wave function, and it is sufficient to take into account only the corrections to the vertices with external probe. This advantage reduces the number of Feynman diagrams dramatically, and makes the calculation of higher order terms very simple.

## 6. Discussion and conclusions

In this work, we employed the pionless EFT with di-baryon fields including the Coulomb interaction, and calculated the analytic expression of the amplitude for the $pp$ fusion process, $pp \to de^+\nu_e$, up to NLO. Employing the assumption to distinguish LO and NLO terms in the contact di-baryon–di-baryon-axial-current interaction, we reproduced the expression for the amplitude of the effective range theory at LO. The LEC $l_{1A}$, which appears in the contact di-baryon–di-baryon-axial-current interaction at NLO, is fixed by using the relative strength of the two-body amplitude to the one-body one, $\delta_{2B}$, which has been determined from the tritium lifetime in the HB$\chi$PT calculation, and thus we could perform the parameter-free-calculation for the $pp$ fusion process. We find that our numerical result of squared reduced amplitude $\Lambda^2(0)$ is in good agreement with those of the recent theoretical calculations within the accuracy better than 1%.

As mentioned in the Introduction, the current theoretical uncertainties for the $pp$ fusion process is ∼0.3% in the HB$\chi$PT calculation up to N$^3$LO [14]. To improve our result to a few tenth% accuracy, it would be essential to include the higher order corrections in the modified counting rules discussed in the neutron beta decay calculation [30]: the next higher order corrections would be the $\alpha$ order and $1/m_N$ corrections. It is known that the higher $\alpha$ order corrections, such as the vacuum polarization effect [9] and the radiative corrections from the one-body part [30],[3] are significant, whereas the corrections from the $1/m_N$ terms would be $p_c/m_N \sim 0.16\%$. It would be worth calculating the $S$ factor for the $pp$ fusion process in a few tenth% accuracy with the pionless EFT with di-baryon fields including those higher order corrections.

Another issue that we would need to clarify is the value of the LEC $l_{1A}$, which has been fixed in this work by using the result from the HB$\chi$PT calculation. As discussed, e.g., in Refs. [14, 35], the LECs which appear in the two-di-baryon-axial-current or four-nucleon-axial-current contact interactions, denoted by $l_{1A}$ in the pionless EFT with di-baryon fields, $L_{1A}$ in the pionless EFT without di-baryon fields, and $\hat{d}^R$ in HB$\chi$PT, are universal. In other words, those LECs are shared by the processes, such as, the $pp$ fusion process ($pp \to de^+\nu_e$) [12–14,16,17], $nn$ fusion process ($nn \to de^-\bar{\nu}_e$) [21], neutrino deuteron reactions ($\nu_e d \to ppe^-$, $\nu_e d \to np\nu_e$) [36,37], muon capture on the deuteron ($\mu^- d \to nn\nu_\mu$) [38, 39], radiative pion capture on the deuteron ($\pi^- d \to nn\gamma$ [40] and its crossed partner $\gamma d \to nn\pi^+$ [41]), tritium beta decay [14], and hep process ($p^3\mathrm{He} \to {}^4\mathrm{He}\, e^+\nu_e$) [14]. If these LECs are determined by using the experimental data from one of the processes, the lattice simulation [42], or the renormalization group method [43], then we can predict the other processes in each of the formalisms without any unknown parameters. In this respect, it may be worth fixing the LEC $l_{1A}$ in the same formalism, the pionless EFT with di-baryon fields, from, e.g., the tritium lifetime extending our formalism to the three-body systems with electroweak external probes.

## Acknowledgements

We would like to thank T.-S. Park for communications and M.C. Birse for reading the manuscript and commenting on it. S.A. is supported by the Korean Research Foundation and the Korean Federation of Science and Technology Societies Grant funded by Korean Government (MOEHRD, Basic Research Promotion Fund): the Brain Pool program (052-1-6) and KRF-2006-311-C00271, and by STFC grant number PP/F000448/1. Work of J.W.S. and S.W.H. is supported by the Korea Science and Engineering Foundation grant funded by the Korean Government (MOST) (No. M20608520001-07B0852-00110). The work of K.K. is supported by the US National Science Foundation under Grant PHY-0457014.

## References

[1] H.A. Bethe, Phys. Rev. 55 (1938) 434.
[2] J.N. Bahcall, Neutrino Astrophysics, Cambridge Univ. Press, Cambridge, 1989.
[3] E.G. Adelberger, et al., Rev. Mod. Phys. 70 (1998) 1265.
[4] K. Kubodera, T.-S. Park, Annu. Rev. Nucl. Part. Sci. 54 (2004) 19.
[5] H.A. Bethe, C.L. Critchfield, Phys. Rev. 54 (1938) 248.
[6] E.E. Salpeter, Phys. Rev. 88 (1952) 547.
[7] E.E. Salpeter, arXiv: 0711.3139.
[8] J.N. Bahcall, R.M. May, Astrophys. J. 155 (1969) 501.

[3] The radiative corrections from the one-body part are quite significant, 2–3% level, and are conventionally included into the renormalized Fermi constant $G'_V \simeq G_F V_{ud}$ and the phase factor $f_{pp}$ in the estimation of the $S$ factor for the $pp$ fusion process.

[9] M. Kamionkowski, J.N. Bahcall, Astrophys. J. 420 (1994) 884.
[10] J. Carlson, et al., Phys. Rev. C 44 (1991) 619.
[11] R. Schiavilla, et al., Phys. Rev. C 58 (1998) 1263.
[12] T.-S. Park, K. Kubodera, D.-P. Min, M. Rho, Astrophys. J. 507 (1998) 443.
[13] T.-S. Park, et al., nucl-th/0106025.
[14] T.-S. Park, et al., Phys. Rev. C 67 (2003) 055206.
[15] J.-W. Chen, G. Rupak, M.J. Savage, Nucl. Phys. A 653 (1999) 386.
[16] X. Kong, F. Ravndal, Nucl. Phys. A 656 (1999) 421;
X. Kong, F. Ravndal, Phys. Lett. B 470 (1999) 1;
X. Kong, F. Ravndal, Phys. Rev. C 64 (2001) 044002.
[17] M. Butler, J.-W. Chen, Phys. Lett. B 520 (2001) 87.
[18] S.R. Beane, M.J. Savage, Nucl. Phys. A 694 (2001) 511.
[19] S. Ando, C.H. Hyun, Phys. Rev. C 72 (2005) 014008.
[20] J. Soto, J. Tarrus, arXiv: 0712.3404.
[21] S. Ando, K. Kubodera, Phys. Lett. B 633 (2006) 253.
[22] S. Ando, R.H. Cyburt, S.-W. Hong, C.H. Hyun, Phys. Rev. C 74 (2006) 025809.
[23] S. Ando, Eur. Phys. J. A 33 (2007) 185, arXiv: 0708.4088.
[24] D.B. Kaplan, Nucl. Phys. B 494 (1997) 471.
[25] F. Gabbiani, nucl-th/0104088;
D.B. Kaplan, J.V. Steele, Phys. Rev. C 60 (1999) 064002.
[26] M. Rho, in: AIP Conference Proceedings, vol. 494, American Institute of Physics, New York, 1999, p. 391, nucl-th/9908015;
D.R. Phillips, T.D. Cohen, Nucl. Phys. A 668 (2000) 45;
D.R. Phillips, G. Rupak, M.J. Savage, Phys. Lett. B 473 (2000) 209.
[27] D.B. Kaplan, M.J. Savage, M.B. Wise, Phys. Lett. B 424 (1998) 390;
D.B. Kaplan, M.J. Savage, M.B. Wise, Nucl. Phys. B 534 (1998) 329.
[28] H.A. Bethe, Phys. Rev. 76 (1949) 38.
[29] L. Durand III, Phys. Rev. 108 (1957) 1597;
L. Heller, Phys. Rev. 120 (1960) 627.
[30] S. Ando, et al., Phys. Lett. B 595 (2004) 250.
[31] X. Kong, F. Ravndal, Phys. Lett. B 450 (1999) 320.
[32] S. Ando, J.W. Shin, C.H. Hyun, S.W. Hong, Phys. Rev. C 76 (2007) 064001.
[33] R.B. Wiringa, V.G.J. Stokes, R. Schiavilla, Phys. Rev. C 51 (1995) 38.
[34] R. Machleidt, Phys. Rev. C 63 (2001) 024001.
[35] A. Gardestig, D.R. Phillips, Phys. Rev. Lett. 96 (2006) 232301.
[36] S. Nakamura, et al., Nucl. Phys. A 707 (2002) 561;
S. Ando, et al., Phys. Lett. B 555 (2003) 49.
[37] M. Butler, J.-W. Chen, Nucl. Phys. A 675 (2000) 575;
M. Butler, J.-W. Chen, X. Kong, Phys. Rev. C 63 (2001) 035501.
[38] S. Ando, et al., Phys. Lett. B 533 (2002) 25.
[39] J.-W. Chen, et al., Phys. Rev. C 72 (2005) 061001.
[40] A. Gardestig, D.R. Phillips, Phys. Rev. C 73 (2006) 014002.
[41] V. Lensky, et al., Eur. Phys. J. A 26 (2005) 107.
[42] W. Detmold, M.J. Savage, Nucl. Phys. A 743 (2004) 170.
[43] M.C. Birse, J.A. McGovern, K.G. Richardson, Phys. Lett. B 464 (1999) 169;
T. Barford, M.C. Birse, Phys. Rev. C 67 (2003) 064006;
S.X. Nakamura, S. Ando, Phys. Rev. C 74 (2006) 034004.